3. Sánchez-Lavega, A. *et al.* Interactions of Jovian White Ovals BC and DE in 1998 from Earth-based observations in the visual range. *Icarus* **142,** 116–124 (1999).
4. Sánchez-Lavega, A. *et al.* The merger of two giant anticyclones in the atmosphere of Jupiter. *Icarus* **149,** 491–495 (2001).
5. Youssef, A. & Marcus, P. S. The dynamics of jovian white ovals from formation to merger. *Icarus* **162,** 74–93 (2003).
6. MacLow, M.-M. & Ingersoll, A. P. Merging of vortices in the atmosphere of Jupiter: an analysis of Voyager images. *Icarus* **65,** 353–369 (1986).
7. Nezlin, M. Rossby solitary vortices, on giant planets and in the laboratory. *Chaos* **4,** 187–202 (1994).
8. Sutyrin, G. Long lived planetary vortices and their evolution: Conservative intermediate geostrophic model. *Chaos* **4,** 203–212 (1994).
9. Marcus, P. S. Numerical simulations of Jupiter's Great Red Spot. *Nature* **331,** 693–696 (1988).
10. Marcus, P. S. Jupiter's Great Red Spot and other vortices. *Annu. Rev. Astron. Astrophys.* **31,** 523–573 (1993).
11. Solomon, T. H., Holloway, W. J. & Swinney, H. L. Shear flow instabilities and Rossby waves in barotropic flow in a rotating annulus. *Phys. Fluids* **5,** 1971–1982 (1993).
12. Marcus, P. S. & Lee, C. A model for eastward and westward jets in laboratory experiments and planetary atmospheres. *Phys. Fluids* **10,** 1474–1489 (1998).
13. Flasar, F. M. Global dynamics and thermal structure of Jupiter's atmosphere. *Icarus* **65,** 280–303 (1986).
14. Gierasch, P. J. Radiative-convective latitudinal gradients for Jupiter and Saturn models with a radiative zone. *Icarus* **142,** 148–154 (1999).
15. Ottino, J. M. *The Kinematics of Mixing: Stretching, Chaos, and Transport* (Cambridge Univ. Press, Cambridge, 1989).
16. Solomon, T. H., Weeks, E. R. & Swinney, H. L. Chaotic advection in a two-dimensional flow: Levy flights and anomalous diffusion. *Physica D* **76,** 70–84 (1994).
17. Panetta, R. L. Zonal jets in wide baroclinically unstable regions: Persistence and scale selection. *J. Atmos. Sci.* **50,** 2073–2106 (1993).
18. Drazin, P. G. & Reid, W. *Hydrodynamic Stability* (Cambridge Univ. Press, Cambridge, 1981).
19. Humphreys, T. D.. *Jovian Kármán Vortex Streets as Attractors in Turbulent Zonal Flow.* Thesis, Univ. California, Berkeley (2000).
20. Dowling, T. E. & Ingersoll, A. P. Jupiter's Great Red Spot as a shallow water system. *J. Atmos. Sci.* **46,** 3256–3278 (1989).
21. Marcus, P. S. Vortex dynamics in a shearing zonal flow. *J. Fluid. Mech.* **215,** 393–430 (1990).
22. Pedlosky, J. *Geophysical Fluid Dynamics* (Springer, New York, 1987).
23. Chandrasekhar, S. *Hydrodynamic and Hydromagnetic Stability* (Oxford Univ. Press, Oxford, 1961).

Supplementary Information accompanies the paper on **www.nature.com/nature**.

Acknowledgements The author thanks T. Kundu for cloud simulations and X. Asay-Davis, S. Shetty and C.-H. Jiang for calculations of temperature changes. The work was supported by the NASA Origins Program, the NSF Astronomy and Plasma Physics Programs and LANL. Computing resources were supplied by NPACI (supported by the NSF).

Competing interests statement The author declares that he has no competing financial interests.

Correspondence and requests for materials should be addressed to the author (pmarcus@me.berkeley.edu).

The ultimate speed of magnetic switching in granular recording media

I. Tudosa[1], C. Stamm[1], A. B. Kashuba[2], F. King[3], H. C. Siegmann[1], J. Stöhr[1], G. Ju[4], B. Lu[4] & D. Weller[4]

[1]*Stanford Synchrotron Radiation Laboratory, PO Box 20450, Stanford, California 94309, USA*
[2]*Landau Institute for Theoretical Physics, Kosygin str. 2, Moscow 117940, Russia*
[3]*Stanford Linear Accelerator Center, Stanford University, Stanford, California 94309, USA*
[4]*Seagate Technology LLC, Pittsburgh, Pennsylvania 15222, USA*

In magnetic memory devices, logical bits are recorded by selectively setting the magnetization vector of individual magnetic domains either 'up' or 'down'. In such devices, the fastest and most efficient recording method involves precessional switching[1–4]: when a magnetic field B_p is applied as a write pulse over a period τ, the magnetization vector precesses about the field until $B_p\tau$ reaches the threshold value at which switching occurs. Increasing the amplitude of the write pulse B_p might therefore substantially shorten the required switching time τ and allow for faster magnetic recording. Here we use very short pulses of a very high magnetic field[5] to show that under these extreme conditions, precessional switching in magnetic media supporting high bit densities no longer takes place at well-defined field strengths; instead, switching occurs randomly within a wide range of magnetic fields. We attribute this behaviour to a momentary collapse of the ferromagnetic order of the spins under the load of the short and high-field pulse, thus establishing an ultimate limit to the speed of deterministic switching and magnetic recording.

Our conceptually simple technique, which could also be used to study the dynamics of ferromagnetic spins underlying many applications and promising developments in magnetism[6–8], utilizes relativistic electron bunches of energy 28 GeV from the Stanford Linear Accelerator to generate unique short and strong magnetic field pulses[5,9]. Our magnetic field resembles the field generated by a straight current-carrying wire, with the familiar closed circular magnetic field lines about the beam direction with the field strength decreasing as $1/R$ with the distance R from the centre of the beam. The electron beam is focused to a cross-section of $10.8 \times 7.4\,\mu$m (full-width at half-maximum) in the x–y plane of the sample surface, perpendicular to the z propagation direction, which lies along the surface normal. Along z, the electron distribution is gaussian with a variance of $\sigma_z = 0.7$ mm in the laboratory frame, giving a pulse duration of $\tau = \sigma_z/c = 2.3 \times 10^{-12}$ s, where c is the speed with which the electrons travel. For all practical purposes that speed is equal to the speed of light.

With the films magnetized perpendicular to the film plane, the magnetic field $\mathbf{B_p}$ and magnetization $\mathbf{M}$ are orthogonal everywhere. This is the optimum geometry to induce a precessional motion of $\mathbf{M}$ about the perpendicular $\mathbf{B_p}$ field, which lies in the magnetically hard plane of the film. Once $\mathbf{M}$ has precessed about $\mathbf{B_p}$ by an angle large enough to cross the hard plane of the sample, it will continue to relax by itself into the opposite direction. Hence in the end it has switched from one easy direction into the opposite easy direction. If however $\mathbf{B_p}$ ceases to exist before $\mathbf{M}$ has reached the hard plane, $\mathbf{M}$ is expected to relax back to its original perpendicular direction, hence no switch is observed. The condition for switching is that the angle of precession $\phi = \omega\tau \geq \pi/2$. As the angular velocity ω is determined by B_p, we obtain the switching condition $B_p\tau \geq$ const.

To test this switching, we prepared 14-nm-thick films of perpendicular granular magnetic recording media of the CoCrPt-type such as recently used in high-density magnetic recording[10]. The main condition for high-density recording is that the grains are decoupled so that the medium can sustain narrow transitions between 'up' and 'down' bits. The decoupling of the grains occurs through segregation of Cr to the grain boundaries induced by deposition at elevated temperature. The grain size was determined by X-ray diffraction to be 20 ± 5 nm. This grain size is so small that the magnetic field B_p is homogeneous over the grain size to better than 0.1% over the R-range of interest. We can then assume that the switching of a grain occurs in a homogeneous applied field. As a substrate, we have used glass with appropriate thin buffer layers, with and without adding a soft magnetic underlayer such as needed in perpendicular recording[10].

The top left panel of Fig. 1 displays contour lines of constant B_p in the film plane. B_p is the peak strength of the gaussian magnetic field pulse calculated from the electron bunch parameters as $B_p = 54.7/R$ where R is measured in micrometres and B_p in tesla. The dark central spot indicates the size of the electron beam focus, close to which no data are obtained owing to beam damage in the sample. The scale is chosen to be the same as in the actual magnetic switching patterns recorded in the other panels of Fig. 1.

Before exposure, the samples were magnetized perpendicular to the film plane into what we shall call the 'up' direction. We recorded patterns on the same sample corresponding to a single shot (pulse),

a pattern corresponding to two shots at the same location, and so on, up to seven consecutive shots per pattern. The time separation of consecutive shots was 1 s. Three weeks after exposure, the perpendicular component of **M** was imaged by polar magneto-optic Kerr microscopy. A set of such images is shown in Fig. 1. The spatial resolution of Kerr microscopy is 1 μm, so that we integrate over 2,500 grains. The spot in the centre of the pattern is due to beam damage. It extends to roughly twice the beam focus. The increase of the damaged area with the number of shots is due to beam jitter, which is estimated to be ±2 μm per shot only. The grey scale of the images is such that the light regions near the edge of the frames correspond to the initial 'up' state. Darkening indicates that particles in the regions have increasingly switched to the 'down' direction.

It is evident that switching occurs along circular contour lines B_p = const., with the contrast changing gradually over a distance of tens of micrometres, rather than abruptly. The switching is not reversible, because the second pulse does not return **M** to the initial 'up' direction. For odd shot numbers, the dark ring where **M** has switched from 'up' to 'down' narrows with increasing number of shots, whereas the outer grey zone corresponding to partially switched **M** expands. With an increasing number of even shots, the central light ring narrows and the outer grey zone expands. This switching behaviour is characteristic of a stochastic process. Starting with a homogeneous magnetic 'up' state, it takes only seven shots to create a random distribution of magnetization directions throughout the large grey zone, where **M** is 'up' in some grains but 'down' in others.

To describe the stochastic switching, consider that the angle ϕ of precession may be short of $\pi/2$ needed for switching. The lacking precessional angle may be supplied by random torques or by random initial conditions. We now assume that the probability p of such stochastic events is gaussian, and can be expressed as the probability density of an additional magnetic field Γ:

$$p(\Gamma) = \frac{1}{\Delta B\sqrt{2\pi}} e^{-\frac{\Gamma^2}{2(\Delta B)^2}}$$

The magnetic order parameter $M(B)$ is given by the fraction of particles that switch minus the fraction of particles that do not

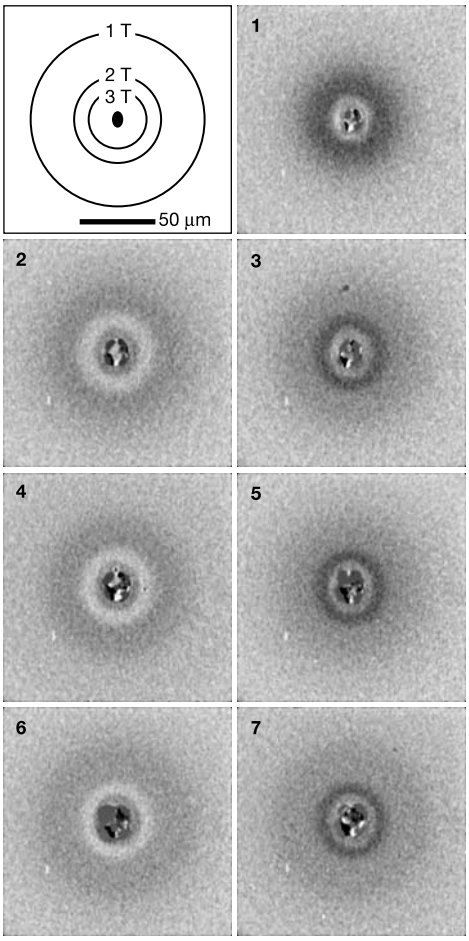

Figure 1 Magneto-optic patterns of magnetization. Diagram at top left, contour lines of constant B_p with area of the electron beam focus in the centre. The numbers on subsequent panels indicate the number of electron bunches (shots) that passed through the sample. Grey contrast is such that the outer light region corresponds to **M** in the initial 'up' state. As darkening intensifies, **M** has switched increasingly to the 'down' direction. The contrast in the central region at $R < 10$ μm is due to beam damage.

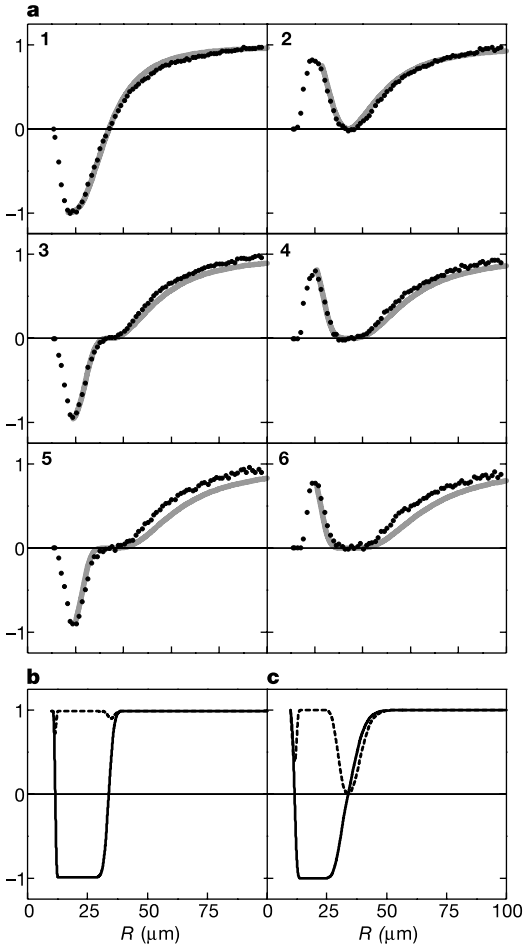

Figure 2 Magnetic order parameter $M_n(R)$. **a**, Data points are from averaged radial cuts of the Kerr images of Fig. 1, setting $M_1(100\,\mu m) = +1$ and $M_1(20\,\mu m) = -1$. The grey lines are generated from $M_n(R) = M_1^n(R)$. **b**, Calculated $M_1(R)$ (full line) and $M_2(R)$ (dashed line) with the observed easy-axis dispersion of 5.5° FWHM[10], showing $M_2(R) \equiv M_o = +1$ in gross contradiction to the experiment. **c**, Calculated $M_1(R)$ (full line) and $M_2(R)$ (dashed line) assuming the excitation of the uniform precession mode (Fig. 3a) corresponding to $K_uV/kT = 40$, where K_u is the uniaxial crystalline anisotropy constant, V the volume of a grain, and kT the Boltzmann factor[12].

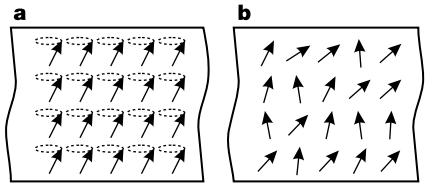

Figure 3 Spin motion in a magnetic grain. **a**, The uniform precession mode of the spins with wavevector $q = 0$. The excitation of this mode determines the long-term stability of the magnetization direction in the grain[12]. **b**, A moment in time with non-uniform excitation of the spins. At ambient temperature, these excitations have small amplitude, which however dramatically increases after the field pulse has been applied. Sizeable exchange fields are generated by the angles between neighbouring spins that can account for the random torques operating after the magnetic field pulse.

switch in a single pulse of amplitude B:

$$M(B) = \int_{-\infty}^{B_0-B} p(\Gamma)\mathrm{d}\Gamma - \int_{B_0-B}^{\infty} p(\Gamma)\mathrm{d}\Gamma$$

By choosing the average switching pulse amplitude $B_o = 1.70\,\mathrm{T}$ and its variance $\Delta B = 0.59\,\mathrm{T}$ we obtain the order parameter $M_1(B_p)$ after the first shot generated from the uniform initial state $M_o = +1$. Substituting the variable B_p by R yields the radial dependence $M_1(R)$ of the magnetization after the first shot. $M_1(R)$ is plotted for $R > 20\,\mu\mathrm{m}$ as a solid line on top of the data points in panel 1 of Fig. 2a. It agrees with the experimental data. The increase of the observed $M_1(R)$ at $R < 20\,\mu\mathrm{m}$ indicates the onset of the second switch where M precessed by $\phi \geq 3\pi/2$. We do not analyse this second switch because it occurs close to the beam damage area.

The other distributions of $M_n(R)$ shown as solid lines in panels 2–6 of Fig. 2a are generated by multiplication $M_n(R) = {}_n(R) = M_{n-1}(R) \times M_1(R) = M_1^n(R)$. This accounts very well for the features observed in the experimental data shown as points in Fig. 2a, despite the fact that raising $M_1(R)$ to the nth power enhances errors. Experimental errors are caused by beam jitter, variations in the number of electrons per bunch, and the uncertainty in the extrapolation of $M_1(R) \rightarrow +1$. At any rate, multiplicative probabilities are the signature of a random variable. Therefore, this analysis reveals that a memory-less process, usually referred to as a Markov uniform stochastic process, dominates the switching.

Different samples have been studied within a range of magnetic parameters such as saturation magnetization and magnetic anisotropy (see Supplementary Information). Information on the switching with older media types such as Co/Pt magnetic multilayers and CoPt alloys is also available[5,9]. The conclusion emerging from all experiments is that stochastic switching is a general feature of ultrafast precessional magnetization reversal.

To explore causes of the randomness, we carried out various calculations using the Landau–Lifshitz–Gilbert (LLG) equation[11]. Theoretical results that explore two hypothetical sources of the randomness are shown in Fig. 2b and c. Figure 2b demonstrates that static dispersion of the easy axis of magnetization in the decoupled grains cannot produce anything but deterministic switching reversing M to the original state $M_o = +1$ in the second shot. This is in gross contradiction to the experiment. Figure 2c explores thermal excitations in terms of the uniform precession mode (illustrated in Fig. 3a). The degree to which the uniform mode is excited is known from the long-term stability of the magnetic bits[12]. It induces randomness in the direction of **M** before the arrival of the field pulse and indeed generates dispersion of $M(R)$, but the dispersion is much too small to explain the data. The effect of heating of the sample by the electron pulse can be asserted without calculation. The supersonic heat wave emerging from the point of beam impact requires 10^{-9} s to travel 1 μm. However, the switching at $R > 20\,\mu\mathrm{m}$ is already completed at that time. Similarly, magneto-static coupling between the grains cannot explain the variance of the switching fields because it is small at the end of the field pulse when the spins have precessed close to the hard plane (see Supplementary Information).

However, the thermal fluctuations within a grain also include higher modes in which the spins are not parallel to each other (illustrated in Fig. 3b). At ambient temperature, these fluctuations have small amplitude. Calculations show that the sharply rising field pulse greatly amplifies the pre-existing thermal randomness. The amplification of the thermal fluctuations leads to the observed variance of the switching fields.

The crystalline magnetic anisotropy $H_A = 1.20 \times 10^6\,\mathrm{A\,m^{-1}}$, the saturation magnetization $M_s = 0.652\,\mathrm{T}$, and the average switching field $B_o = 1.7\,\mathrm{T}$ are compatible with the LLG equation if the damping of the magnetization precession in a grain is assumed to be $\alpha = 0.3$. This extremely large damping shows that torque is lost at a high rate to the spin system, proving indeed the excitation of spin fluctuations. It is well known that the spin system is pushed easily into auto-oscillation and chaos as the absorbed power increases[13,14]. At the end of the field pulse, the non-equilibrium modes illustrated in Fig. 3b exert the postulated random torques. We therefore believe that our experiment reveals 'fracture of the magnetization' under the load of the fast and high field pulses, putting an end to deterministic switching as we know it today. □

Received 4 July 2003; accepted 25 February 2004; doi:10.1038/nature02438.

1. Gerrits, Th. *et al.* Ultrafast precessional magnetization reversal by picosecond magnetic field pulse shaping. *Nature* **418,** 509–511 (2002).
2. Hiebert, W. K., Ballentine, G. E. & Freeman, M. R. Comparison of experimental and numerical micromagnetic dynamics in coherent precessional switching and modal oscillations. *Phys. Rev. B* **65,** 140404(R) (2002).
3. Kaka, S. & Russek, S. E. Precessional switching of submicrometer spin valves. *Appl. Phys. Lett.* **86,** 2958–2960 (2002).
4. Schumacher, H. W. *et al.* Phase coherent precessional magnetization reversal in microscopic spin valve elements. *Phys. Rev. Lett.* **90,** 017201 (2003).
5. Siegmann, H. C. *et al.* Magnetism with picosecond field pulses. *J. Magn. Magn. Mater.* **151,** L8–L12 (1995).
6. Rhie, H.-S., Dürr, H. A. & Eberhardt, W. Femtosecond electron and spin dynamics in Ni/W(110) films. *Phys. Rev. Lett.* **90,** 247201 (2003).
7. Kiselev, S. I. *et al.* Microwave oscillations of a nanomagnet driven by a spin-polarized current. *Nature* **425,** 380–383 (2003).
8. Urazhdin, S. *et al.* Current-driven magnetic excitations in permalloy-based multilayer nanopillars. *Phys. Rev. Lett.* **91,** 146803 (2003).
9. Back, C. H. *et al.* Magnetization reversal in ultrashort magnetic field pulses. *Phys. Rev. Lett.* **81,** 3251–3254 (1998).
10. Lu, B. *et al.* High anisotropy CoCrPt(B) media for perpendicular magnetic recording. *J. Appl. Phys.* **93,** 6751–6753 (2003).
11. Hillebrands, B. & Ounadjela, K. (eds) *Spin Dynamics in Confined Magnetic Structures I* (Springer, Berlin, 2002).
12. Weller, D. & Moser, A. Thermal effect limits in ultrahigh-density magnetic recording. *IEEE Trans. Magn.* **35,** 4423–4439 (1999).
13. Ebels, U., Buda, L. D., Ounadjela, K. & Wigen, P. E. in *Spin Dynamics in Confined Magnetic Structures I* (eds Hillebrands, B. & Ounadjela, K.) 178–181 (Springer, Berlin, 2002).
14. Safonov, V. L. & Bertram, H. N. Spin-wave dynamic reversal in a quasi-single domain magnetic grain. *Phys. Rev. B* **63,** 094419 (2001).

Supplementary Information accompanies the paper on **www.nature.com/nature**.

Acknowledgements We thank R. Iverson, C. Field and G. J. Collet for their assistance in preparing and carrying out the sample exposure at FFTB, and A. Vaterlaus for help with imaging the magnetic patterns. This work was carried out at the Stanford Linear Accelerator Center, which is supported by the Office of High Energy and Nuclear Physics of the US Department of Energy (DOE). The experimental programme of the SSRL authors is funded by the Office of Basic Energy Sciences of DOE.

Competing interests statement The authors declare that they have no competing financial interests.

Correspondence and requests for materials should be addressed to J.S. (stohr@slac.stanford.edu).